BMC Genomics

RESEARCH Open Access

Integrated transcriptomic and metabolomic analyses reveal the mechanism of shoot growth in grafted *Camellia oleifera* seedlings

Yayan Zhu[1†], Chaoran Xu[1†], Feng Xiao[2], Fang Li[1], Qinmeng Zeng[1], Yingying Wei[1] and Jie Xu[1*]

Abstract

Shoot flushing is a critical determinant of grafted seedling quality in *Camellia oleifera*, with key evaluation metrics including flushing timing, new shoot number and growth rate, and seedling height uniformity. To elucidate the molecular mechanisms governing shoot development, we conducted integrated analyses of endogenous hormones, metabolomics, and transcriptomics across three *Camellia* species (*C. oleifera*, *C. meiocarpa*, and *C. weiningensis*). Hormonal profiling revealed that shoot-flushing plants exhibited elevated levels of GA24, GA9, salicylic acid, IAA, IAAla, IPA, and abscisic acid compared to non-flushing plants, while DZ, tZ, and tZR levels were reduced. Metabolomic analysis identified 89 commonly differentially abundant metabolites among the three species. KEGG enrichment and correlation analyses demonstrated significant enrichment of these differentially abundant metabolites and differentially expressed genes in phenylpropanoid biosynthesis, plant hormone signal transduction, and flavonoid biosynthesis pathways. Collectively, our findings indicate that shoot flushing is coordinately regulated by multiple metabolic pathways—including plant hormone signal transduction, phenylalanine metabolism, nitrogen metabolism, phenylpropanoid biosynthesis, and flavonoid biosynthesis—along with expression modulation of key genes such as *PAL6*, *CYP73A4*, *PER42*, *GH3.6*, and *LAX2*. These results provide novel insights into the molecular basis of shoot development and offer potential targets for improving grafted seedling quality in *C. oleifera*.

Keywords *Camellia oleifera*, Shoot flushing, Transcriptome, Metabolome

Introduction

Camellia oleifera, endemic to China, is a woody edible oil tree species with high unsaturated fatty acid content in its seed oil. Apart from the oil, the seed cake and fruit shells of *C. oleifera* have significant utilization value [1, 2]. Cotyledonary-stage rootstock grafting is the primary method for clonal propagation of *C. oleifera*, with numerous studies conducted on key techniques for seedling cultivation through this method [3, 4]. Current research indicates that the growth of *C. oleifera* seedlings is influenced by the interaction between scion and rootstock, with self-rootstock grafting showing higher survival rates [5]. Heterografting suppresses the growth vigor of *C.*

†Yayan Zhu and Chaoran Xu contributed equally to this work and should be considered as co-first authors.

*Correspondence:
Jie Xu
404715698@qq.com
[1]Guizhou Academy of Forestry, Guiyang, Guizhou 550005, China
[2]Institute for Forest Resources and Environment of Guizhou, Guizhou University, Guiyang 550025, China

oleifera, and multi-omics analyses have revealed that heterografting significantly affects the differential expression of key genes (*aroD*, *aroE*, *aroK*, *pheA*, *tyrB*) involved in shikimate and phenylethylamine biosynthesis. Additionally, *AP2/ERF*, *MYB*, and *GRAS* transcription factors are involved in regulating the expression of these key genes [6]. Different combinations of scions and rootstocks have significant impacts on graft survival rates, shoot flushing rates, seedling height, ground diameter, new shoot length, and the growth and morphology of stems, leaves, and roots of grafted plants [7, 8]. The degree of lignification of scion branches and the grafting method have extremely significant or significant effects on the shoot flushing and non-emergence rates of grafted *C. oleifera* seedlings, with shoot flushing rates of 92.00% and 79.33% for recently lignified and semi-lignified branches, respectively [9]. Grafting with medium-sized seeds as rootstocks results in the highest survival rate of 79.9%, while later grafting times lead to lower survival rates; however, the size of the leaf area retained on scion branches has little impact on survival rates and growth factors. Scion branches taken from the upper part of mother trees exhibit significantly different survival rates, shoot lengths, and shoot thickness compared to those from the middle and lower parts [10]. Seedlings grafted with apical, middle, and basal buds show differences in height, with the height order being apical > middle > basal, although the reduction in bud position does not significantly affect plant growth; variety is a critical factor influencing growth [11, 12]. Auxins, cytokinins and strigolactones are three classes of hormones that regulate bud activation and thereby regulate shoot branching [13]. Plant regeneration involves complex transcriptional regulatory networks, among which *WIND1* has been identified as a key regulatory gene for wound-induced cell reprogramming in plants. In *Arabidopsis*, *WIND1* promotes callus formation and shoot regeneration by directly upregulating the expression of *ESR1*, which in turn regulates genes such as *CUC1/2*, *ESR2*, *AHP6*, *CLV3*, *WUS*, *STM*, and *SAM* [14, 15]. Differentially expressed genes (DEGs) related to phenylpropanoid biosynthesis, plant hormone biosynthesis and signal transduction, sucrose and starch metabolism, and MAPK signaling pathways are involved in the healing process of lychee grafting [16].

Preliminary field surveys conducted by our research team in *C. oleifera* nurseries across YuPing, LiPing, CeHeng, GuiYang, and other regions of Guizhou Province revealed substantial variation in shoot flushing rates among different *C. oleifera* varieties grafted onto cotyledonary-stage rootstocks. The shoot flushing rate ranged widely from 6.25% to 100%, and significant differences were observed in the height and collar diameter of two-year-old seedlings. Low shoot flushing rates result in high variability in seedling height, inconsistent seedling quality, and substantially increased nursery production costs and management difficulties. In recent years, integrated metabolomic and transcriptomic analyses have flushing as a powerful approach in multi-omics research, widely applied to studies on plant physiological and biochemical mechanisms, flower coloration and nutrient biosynthesis, and responses to abiotic and biotic stresses [17–20]. By identifying differentially accumulated metabolites and differentially expressed genes, this integrative strategy enables comprehensive and systematic characterization of metabolic accumulation and gene expression patterns, thereby uncovering underlying gene regulatory networks and metabolic pathways [6]. In this study, we performed endogenous hormone profiling, transcriptomic, and metabolomic analyses on grafted plants of *C.oleifera*, *C.meiocarpa*, and *C.weiningensis*—comparing shoot-flushing (branch) and non-flushing (bud) plants—to investigate key physiological factors governing shoot flushing. We aimed to identify critical DEGs and metabolites associated with shoot flushing in grafted *C. oleifera* seedlings and to provide initial insights into the molecular regulatory mechanisms underlying shoot flushing in cotyledonary-stage rootstock grafting.

Results

Analysis of endogenous hormone content

Endogenous hormone analyses of bud and branch revealed that the concentrations of GA24 and GA9, SA, IAA, IAAla, IPA, and ABA were all higher in shoot-flushing plants (branch) than in non-flushing plants (bud) (Fig. 1a to g). Specifically, the average IAA content was 0.0308 ng/mg in Cm branch, 0.0168 ng/mg in Co branch, and 0.0228 ng/mg in Cw branch, while IAA levels in buds were 0.0047 ng/mg (Cm bud), 0.0055 ng/mg (Co bud), and 0.0076 ng/mg (Cw bud), respectively (Fig. 1e). In all cases, IAA concentrations in shoot-flushing plants were significantly higher than those in non-flushing plants. Furthermore, the average GA24 content in shoot-flushing plants was 27.142-fold higher than in non-flushing plants; ABA levels were 4.127-fold higher, and salicylic acid concentrations were 1.940-fold higher. Analysis of cytokinins, including DZ, tZ and tZR, revealed that the concentrations in branch were higher than those in bud (Fig. 1h to j). Specifically, the average tZ content in Cw bud was 0.0022 ng/mg, whereas it was 0.0009 ng/mg in Cw branch (Fig. 1i).Traits within the same group exhibited similar distributions, with the Cm branch group showing a closer correlation to GA9 and IAA (Fig. 1k).

Non-targeted metabolomics analysis

Metabolomics analysis of the samples based on KEGG annotation revealed that Amino acids and Oligosaccharides had more annotations (Fig. 2a). Compound annotations based on HMDB showed that Phenylpropanoids

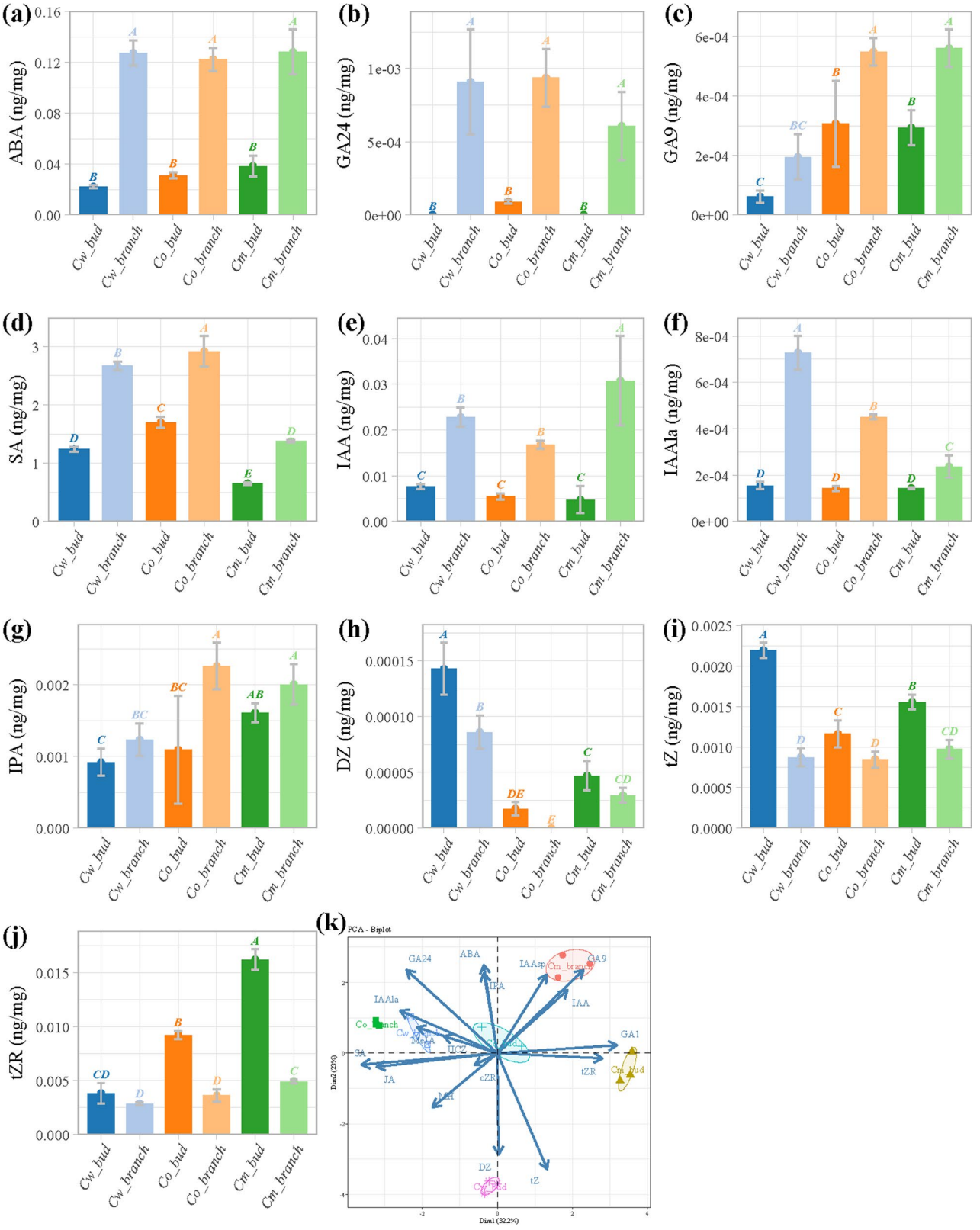

Fig. 1 Changes in endogenous hormone levels in bud and branch of different *Camellial* species. **a**: ABA content; **b**: GA24 content; **c**: GA9 content; **d**: SA content; **e**: IAA content; **f**: IAAla content; **g**: IPA content; **h**: DZ content; **i**: tZ content; **j**: tZR content; **k**: PCA analysis of different grafting combinations. Co: *Camellia oleifera*; Cm *Camellia meiocarpa*; Cw: *Camellia weiningensis*

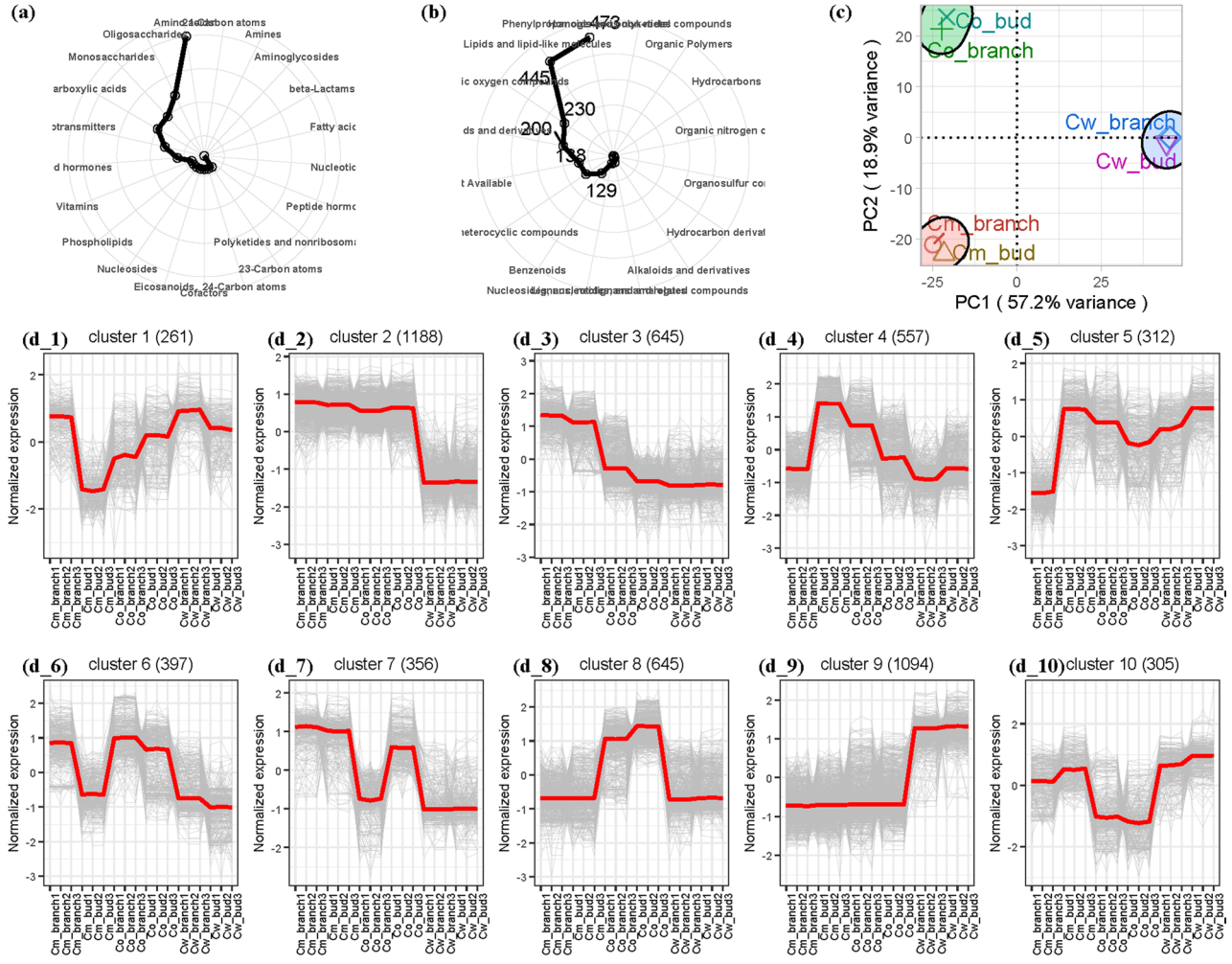

Fig. 2 Trends of non-targeted metabolites in different *Camellia* species. (**a**): Annotation information based on KEGG Compound level-2 classification; (**b**): HMDB compound classification; (**c**): Principal component analysis (PCA); (**d**1–**d**10): Cluster submodules from mfuzz clustering. Notes: In panel (**a**), compound categories with counts exceeding 10 are labeled; in panel (**b**), categories with more than 100 compounds are labeled. In panel (**c**), different background colors represent different sample groups. In panels (**d**1–**d**10), mfuzz clustering was used with the cluster number set to 10; the red line indicates the mean expression trend for each cluster, and each gray line represents an individual metabolite. Co: *C. oleifera*; Cm: *C. meiocarpa*; Cw: *C. weiningensis*

and polyketides (473) and Lipids and lipid-like molecules (445) were the most diverse categories (Fig. 2b). The first principal component (PC1) and the second principal component (PC2) of PCA accounted for 57.2% and 18.9% of the total variance, respectively (Fig. 2c). A total of 2,131 metabolites were annotated across all samples. Using *P*_value < 0.05, VIP > 1, and Fold Change > 15 as thresholds to screen differential metabolites in tested samples, it was found that in Co branch_vs_Co bud, 315 differential metabolites were up-regulated (51.64%) and 295 were down-regulated (48.36%). In Cm branch_vs_Cm bud, 259 differential metabolites were up-regulated (39.78%) and 392 were down-regulated (60.22%). In Cw branch_vs_Cw bud, 248 differential metabolites were up-regulated (40.59%) and 363 were down-regulated (59.41%). Venn diagram analysis revealed that there were 89 common differential metabolites among the three groups. KEGG enrichment analysis of differential metabolites showed that in Co branch_vs_Co bud, mainly including flavone and flavonol biosynthesis ($p = 9.31751678798e-07$, Corrected *P*-Value = 5.31098456915e-05), plant hormone signal transduction (map04075) ($p = 0.0007340579757$, *Corrected P-Value* = 0.0209206523074). Salicylic acid and GA3 were significantly up-regulated in flushed samples, with 4-hydroxycinnamic acid being up-regulated by 2.660-fold. Trend analysis of inter-group differential metabolites between buds and branches revealed specific substances with relatively high expression levels among species, such as 1,188 metabolites in cluster 2 showing relatively high expression in Cm and Co (Fig.2d_2), and 645 metabolites in cluster 8 showing relatively high expression in Co (Fig. 2d_8).

Transcriptome analysis

Transcriptome analysis was performed on 18 samples. All samples yielded clean data exceeding 5.98 Gb, with Q30 bases above 95.18% and GC content ranging from 44.82% to 52.03%. Clean reads from each sample were aligned to the reference genome, achieving alignment rates between 74.09% and 88.45%. A sample correlation heatmap (Fig. 3a) indicated high within-group correlations and good reproducibility. Principal component analysis (PCA) revealed that PCA1 and PCA2 explained

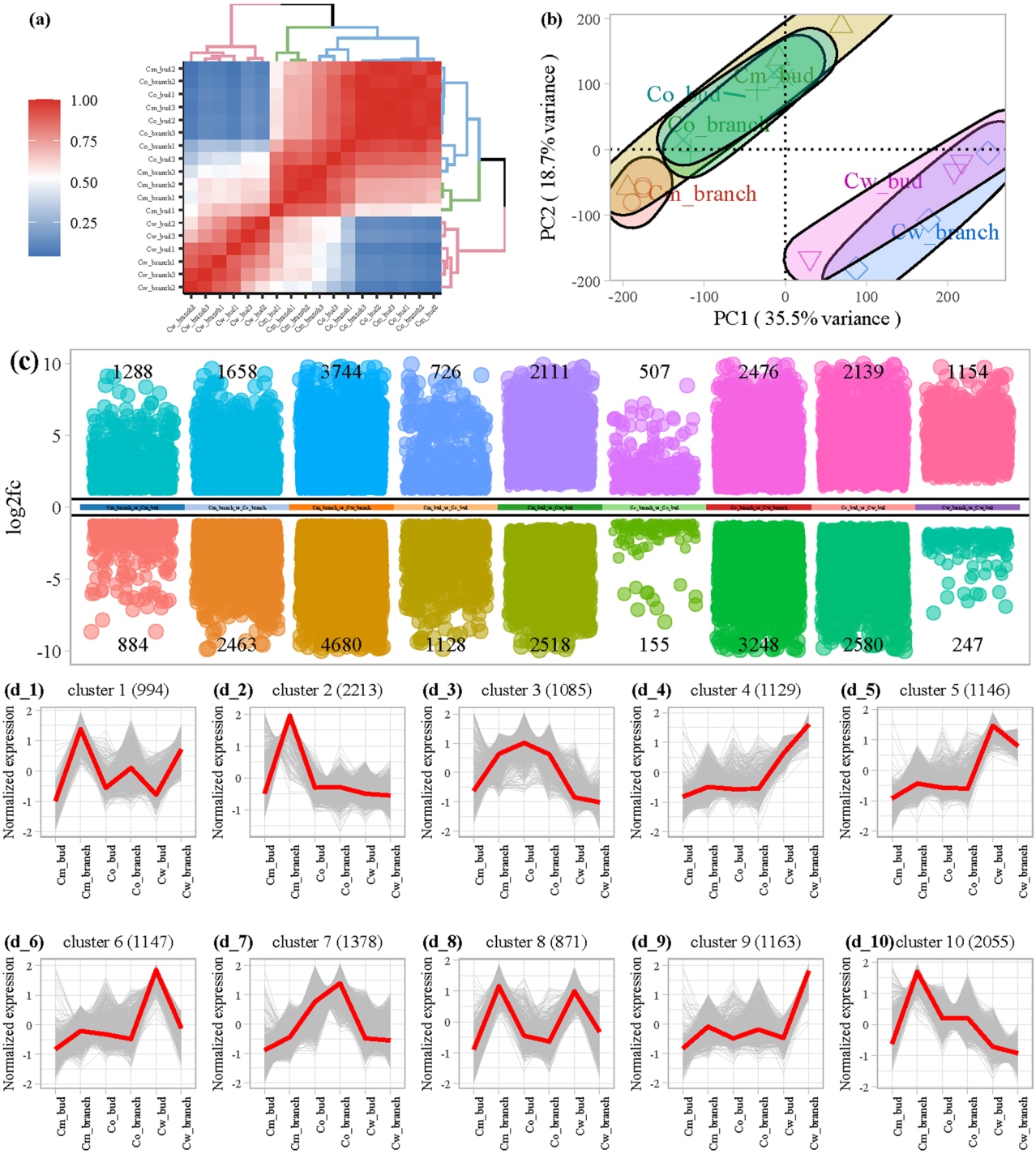

Fig. 3 Transcriptional expression trends in different *Camellia species*. (**a**) Inter-sample correlation analysis; (**b**) Principal component analysis (PCA) of samples; (**c**) Number of differentially expressed genes (DEGs) among different comparisons; (**d**1–**d**10) Cluster submodules from mfuzz clustering. Note: In panels (**d**1–**d**10), mfuzz clustering was used with the cluster number set to 10; the red line represents the average expression trend for each cluster, and each gray line corresponds to an individual gene. Co: *C. oleifera*; Cm: *C. meiocarpa*; Cw: *C. weiningensis*

35.5% and 18.7% of the total variance, respectively (Fig. 3b). Differentially expressed genes (DEGs) between groups were identified based on gene expression quantification, using the criteria $|\log_2 FC| \geq 1$ and adjusted *p*-value (*p* adjust) < 0.05. In Co branch_vs_Co bud, 662 DEGs were identified, including 507 up-regulated and 155 down-regulated genes. In Cm branch_vs_Cm bud, 1,288 genes were up-regulated and 884 were down-regulated. In Cw branch_vs_Cw bud, 1,154 genes were up-regulated and 247 were down-regulated. Venn diagram analysis of DEGs across the three comparisons revealed 156 common DEGs shared among all groups. Cluster analysis of DEGs from different comparisons (Fig. 3d) further showed transcriptional expression patterns with species-specific or tissue-specific high expression trends.

WGCNA analysis

WGCNA co-expression network analysis identified 10 modules significantly associated with traits: the darkturquoise module was significantly positively correlated with salicylic acid (SA) ($r = 0.75$, $p = 0.00033$), and its associated genes were relatively highly expressed in Co; the brown module showed a significant positive correlation with N-(3-Indolylacetyl)-L-alanine (IAAla) ($r = 0.80$, $p = 6.2 \times 10^{-5}$), with its related genes relatively highly expressed in Cw; and the greenyellow module was significantly positively correlated with IAA ($r = 0.76$, $p = 0.00027$) (Fig. 4a-k), with its associated genes relatively highly expressed in Cm. Genes with high intramodular connectivity included *SLC2*, *EREBP*, and *AOC* in the darkturquoise module (Fig. 4l); *E5.2.1.8* and *E3.3.1.1* in the brown module (Fig. 4m); and *CYP73A* in the greenyellow module(Fig. 4n).

Integrated transcriptomic and metabolomic analysis

Venn analysis was performed on the differentially abundant metabolites and differentially expressed genes from three combinations based on KEGG annotation. Both gene sets and transcript sets were jointly annotated to 15 pathways, including Phenylalanine metabolism (map00360), Nitrogen metabolism (map00910), Phenylpropanoid biosynthesis (map00940), Flavonoid biosynthesis (map00941), and ABC transporters (map02010). Among these, significant enrichment was observed in pathways such as Phenylpropanoid biosynthesis, Plant hormone signal transduction (map04075), and Flavonoid biosynthesis.

Measurements of endogenous hormone levels showed that concentrations of GA24, GA9, SA, IAA, IAAla, IPA, and ABA were all significantly higher in shoot-flushing plants than in non-flushing plants.In the metabolome, SA levels were upregulated by 1.298-fold, JA by 1.969-fold, and jasmonoyl-L-isoleucine by 1.426-fold. Additionally, transcriptome sequencing revealed varying degrees of upregulation of several key genes: auxin-amido synthetase genes *GH3.1* and *GH3.6*, auxin influx carrier genes *LAX2* and *LAX4*, and cyclin-encoding genes *CYCD3-1* and *CYCD3-3*. *CYCD3* genes are critical regulators of cell cycle progression, and their upregulated expression may promote cell division and rapid shoot growth. The xyloglucan endotransglucosylase/hydrolase-related gene *XTH23* was also markedly upregulated. Furthermore, pathogenesis-related proteins *PR1B1* and *CAP PR-1* were upregulated, with *CAP PR-1* showing a dramatic 26.437-fold increase.

In the flavonoid biosynthesis pathway, a comparison between shoot-flushing and non-flushing plants of *C. oleifera* revealed significant upregulation in the levels of isosakuranetin, leucocyanidin, vitexin, taxifolin, and epigallocatechin. In contrast, eriodictyol content was downregulated, and quercetin was significantly decreased by 0.713 fold. Concurrently, genes encoding key enzymes in this pathway-including shikimate O-hydroxycinnamoyltransferase (*HST*), shikimate O-acetyltransferase (*SAT*), and leucoanthocyanidin dioxygenase (*LDOX*)-were upregulated to varying degrees.

In the phenylpropanoid biosynthetic pathway, L-tyrosine, L-phenylalanine, and 4-hydroxycinnamic acid (upregulated by 2.660-fold) were differentially upregulated in flushing shoots. Transcriptomic analysis revealed that genes encoding phenylalanine ammonia-lyase (*PAL6*), peroxidases (*PER42*, *PER43*, and *PER72*), as well as cytochrome P450 family members *CYP98A2*, *CYP75A1*, and *CYP73A4* were significantly upregulated in flushing shoots. Notably, *CYP73A4* exhibited a 3.613-fold increase in expression. These findings suggest that the phenylpropanoid biosynthetic pathway may influence shoot growth and development during flushing by coordinately regulating the synthesis of relevant metabolites and the expression of associated genes (Fig. 5).

RT-qPCR validation

To validate the reliability of the transcriptome sequencing data, eight genes associated with shoot flushing in *C. oleifera* were selected from the RNA-seq dataset for quantitative real-time PCR analysis. The expression trends of these eight genes were largely consistent between the transcriptome data and the qRT-PCR results (Fig. S1), indicating high reliability of the RNA-seq data.

Discussion

Shoot flushing is a crucial component of plant growth, closely related to the plant's growth and development as well as its adaptation to the environment. The regulation mechanism of plant growth is complex, involving the coordinated actions of various hormones such as auxins, gibberellins, jasmonic acid, and cytokinins, all of which play roles in regulating axillary bud growth and secondary

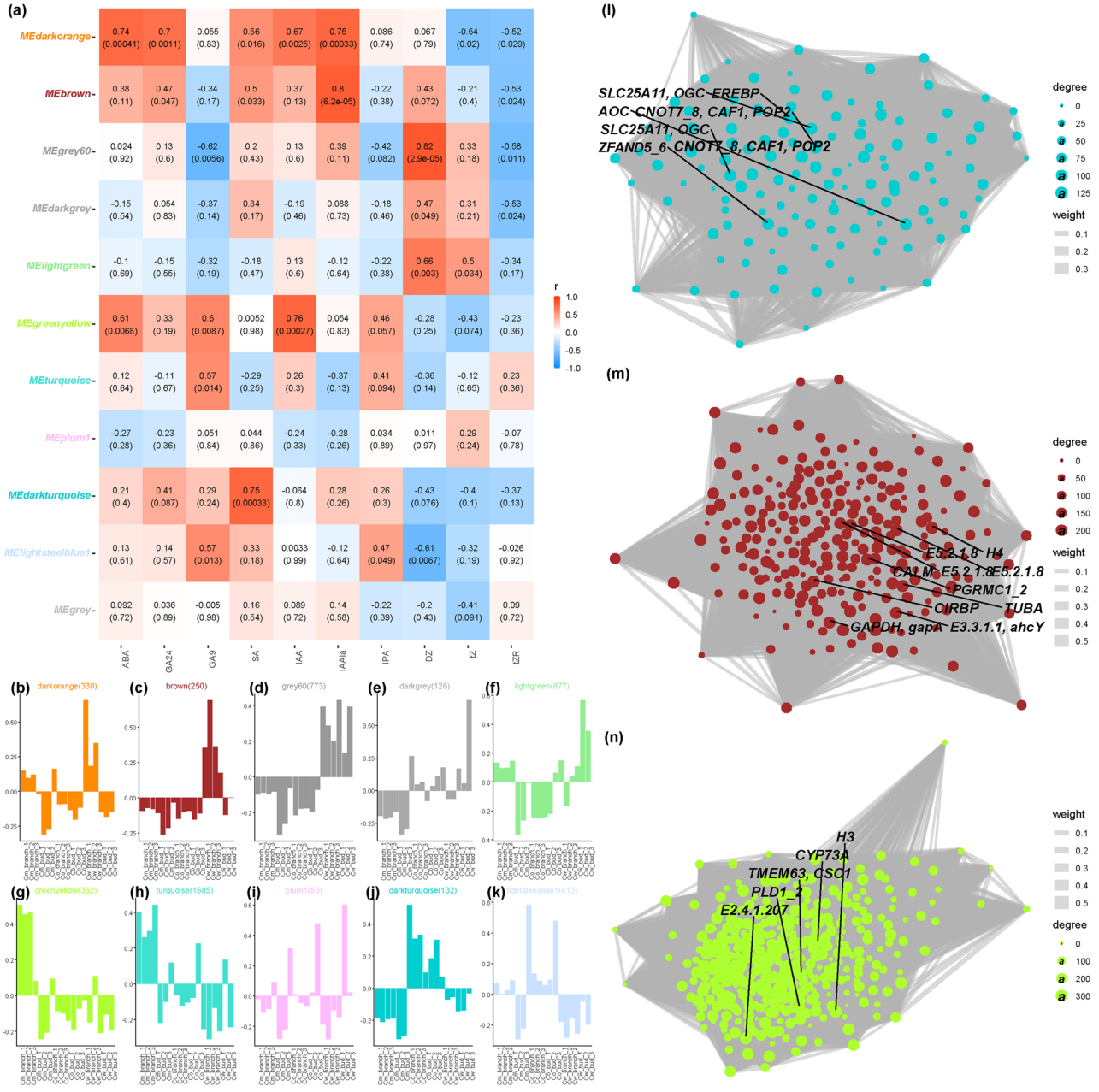

Fig. 4 WGCNA analysis. **a**: Correlation between modules and traits; **b**-**k**: Expression profiles of module eigengenes; **l**: Network visualization of the dark-turquoise module; m: Network visualization of the brown module; **n**: Network visualization of the greenyellow module. Notes: In panel **a**, the correlation coefficients and corresponding *p*-values between modules and various traits are displayed in each grid. The left panel shows different colored modules (with the grey module representing genes that cannot be assigned to any specific module), while the right color scale indicates module-trait correlations ranging from − 1 (blue) to 1 (red). In panels **l**-**n**, the layout output used "fr" (Fruchterman-Reingold layout), and degree was calculated using centrality_degree. The top 20 KO names based on degree are annotated

stem growth [21]. Studies on new shoot growth in *C. sinensis* have found that exogenous application of GA and IAA increases new shoot growth, with the flavonoid biosynthesis pathway being significantly enriched among differentially expressed genes following IAA treatment [22]. Endogenous hormone measurements in branch and bud of *C. oleifera* revealed that levels of GA24 and GA9, SA, IAA, IAAla, and IPA were higher in branch compared to bud. Exogenous hormone treatments of scions indicated that applying appropriate concentrations of IAA, GA3, and NAA before grafting effectively increased graft survival rates and flushing rates, promoting shoot growth [23]. ABA plays an important role in plant growth, development, and stress responses; it is generally considered an inhibitor of axillary bud growth [24]. In *Arabidopsis*, ABA may inhibit bud growth by

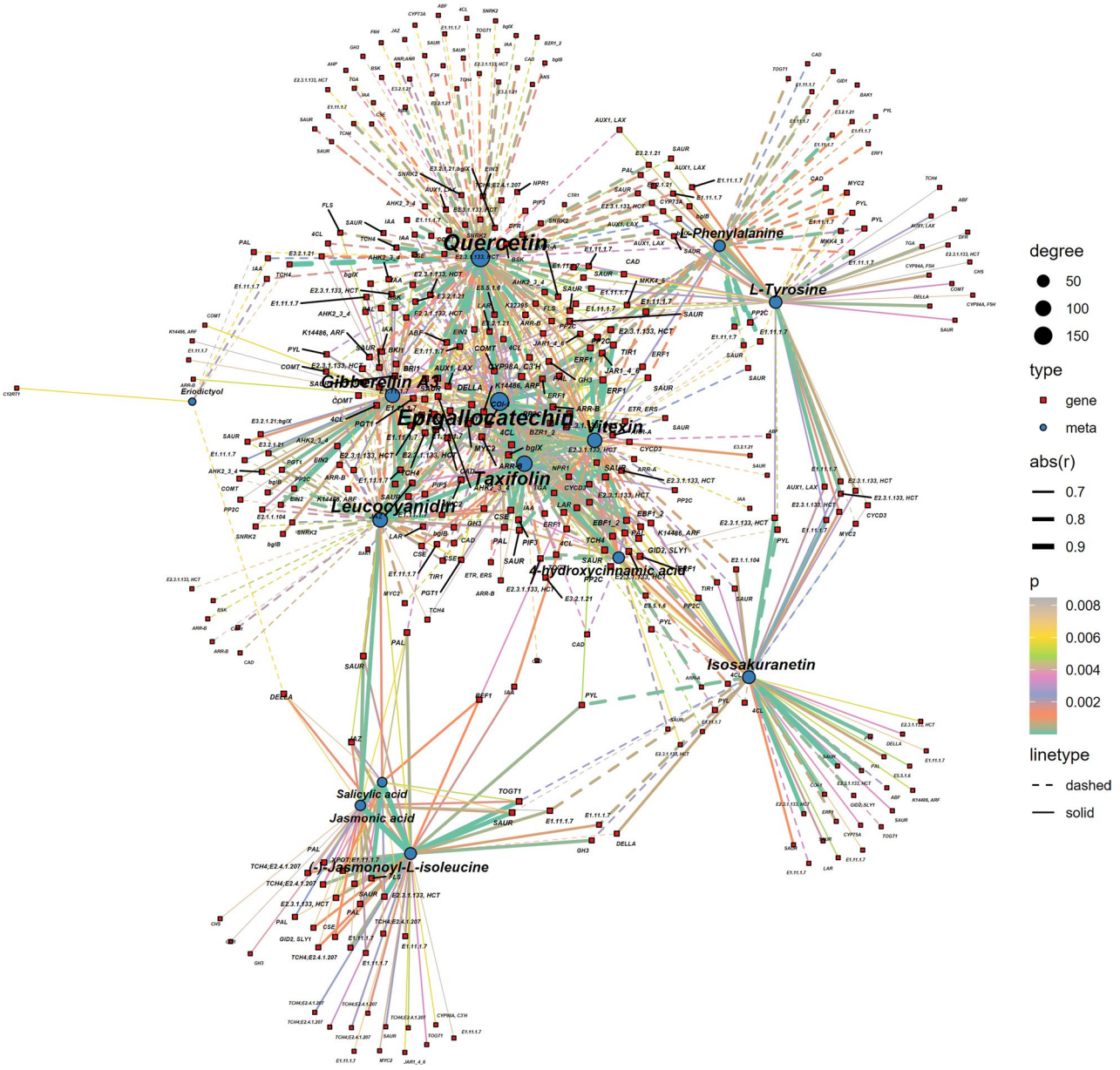

Fig. 5 Network analysis of differentially expressed genes and metabolites. Note: Different shapes represent different types—circles denote metabolites and squares denote genes; solid lines indicate positive correlations, while dashed lines indicate negative correlations. Significant associations were filtered using a threshold of $|r| > 0.6$ and $p < 0.05$

suppressing the cell cycle machinery and bud-autonomous IAA accumulation [24]. However, measurements of endogenous hormones found that average ABA contents in banch of *C. oleifera*, *C. meiocarpa*, and *C. weiningensis* were 0.1224 ng/mg, 0.1282 ng/mg, and 0.1274 ng/mg respectively, all higher than those in bud (0.0311 ng/mg, 0.0384 ng/mg, and 0.0221 ng/mg respectively).This suggests that the increased ABA content may be associated with the larger number of axillary buds in flushing plants, where ABA inhibits the germination of axillary buds rather than the sole bud in non-flushing plants. Additionally, ABA has been shown to regulate adaptive responses to abiotic environmental stresses by activating defense genes within the plant and enhancing disease resistance. Research indicates that exogenous application of ABA can effectively reduce early blight in tomato plants [25]. Integrated analysis with transcriptomic data revealed that defense-related regulatory genes, such as *PR1B1* and *CAP PR-1*, were up-regulated, with *CAP PR-1* showing a 26.437-fold increase. Given that the SA signaling pathway plays a crucial role in regulating *PR1B1* expression, it is hypothesized that the elevated levels of ABA and SA are associated with stress resistance. It has been known that auxin inhibits the activation of axillary buds, and hence

shoot branching, while cytokinin has the opposite effect [26]. Cytokinins are widely recognized as one of the most effective hormones for promoting axillary bud activation, playing a pivotal role in breaking bud dormancy and activating the shoot apical meristem, which is crucial for plant morphogenesis and yield formation [27, 28]. However, quantitative analysis of cytokinins—including DZ, tZ, and tZR-revealed that their concentrations in flushing shoots were lower than those in non-flushing buds, exhibiting a trend opposite to that of IAA.

The phenylpropanoid pathway influences many important traits in plants by synthesizing various secondary metabolites such as lignin and flavonoids. Many natural metabolic products in plants, including phenylpropanoids, terpenoids, alkaloids, fatty acids, and precursors of phytohormones, involve cytochrome P450 monooxygenases in their biosynthesis [29]. P450 enzymes are widely present in various organs and cells of plants, playing a crucial role in plant growth, development, physiological and ecological functions, and stress resistance [30, 31]. Transcriptomic results from shoot-flushing plants and non-flushing plants of *C. oleifera*, *C. meiocarpa*, and *C. weiningensis* indicated that genes from the P450 family, including *CYP77A2*, *CYP716A44*, *CYP73A4*, and *CYP78A9*, were upregulated to varying degrees. Specifically, *CYP73A4* and *CYP78A9* were upregulated by 3.613-fold and 3.842-fold, respectively, with *CYP78A9* showing significant upregulation. Enzymes of the *CYP98A* family play a vital role in phenylpropanoid and lignin biosynthesis pathways; their function is not limited to the direct synthesis of caffeoyl ester derivatives but has a significant impact on plant growth and development [32]. A previous study revealed that overexpression of *CYP98A22* positively affects the concentration of furanocoumarins in *Ruta graveolens* [33]. Cinnamate 4-hydroxylase (*C4H*; *CYP73A*), associated with the endoplasmic reticulum of plant cells, hydroxylates cinnamic acid to form 4-coumaric acid in phenylpropanoid metabolism [34]. Metabolomic results showed that 4-hydroxycinnamic acid was significantly upregulated, likely regulated by *CYP73A4.* Further research into the role of plant P450 enzymes in shoot flushing could uncover the regulatory mechanisms of P450-related genes.

Conclusions

Metabolic pathways—including phenylalanine metabolism, nitrogen metabolism, phenylpropanoid biosynthesis, and flavonoid biosynthesis—along with expression changes in related genes such as *PAL6*, *CYP73A4*, and *PER42*, collectively regulate the process of shoot growth. Plant hormone signal transduction plays a central role in this regulation: genes such as *GH3.1*, *GH3.6*, *LAX2*, and *LAX4* modulate the levels and signaling of hormones including auxin, gibberellins, cytokinin, salicylic acid, and jasmonic acid, thereby influencing multiple physiological processes—such as cell cycle progression, cell wall remodeling, and lignin biosynthesis—and ultimately orchestrating shoot flushing and growth in *C. oleifera*.

Materials and methods

Materials

The experimental materials were obtained from the nursery of the Guizhou Academy of Forestry Sciences. At 16 weeks after grafting, healthy plants of *C. oleifera*, *C. meiocarpa*, and *C. weiningensis* with identical scion–rootstock combinations were selected, including shoot-flushing (branch) and non-flushing (bud) plants (Fig. 6). Stem segments were excised, rinsed thoroughly with deionized water, immediately frozen in liquid nitrogen, and stored at – 80 °C for subsequent analysis. Three biological replicates were prepared for each sample type.

Targeted measurement and analysis of endogenous hormones

Weigh 100 mg of the aforementioned sample, place it in a 2 mL grinding tube, add 498 µL of 80% methanol and 2 µL of SA-D4 internal standard solution (2 µg/mL), grind at low temperature, then add EN15662 (which includes magnesium sulfate 4 g, sodium chloride 1 g, sodium citrate dihydrate 1 g, disodium hydrogen citrate sesquihydrate 0.5 g) for extraction. Qualitative and quantitative detection of the target substances in the samples is performed using LC-ESI-MS/MS (UHPLC-Qtrap). The specific parameters are as follows: Waters BEH C18 (2.1 * 100 mm, 1.7 µm) HPLC column, column temperature 40 °C, injection volume 5 µL. Mobile phase A (2 mM ammonium formate + 0.05% formic acid water), mobile phase B (2 mM ammonium formate + 0.05% formic acid methanol), acquisition time 15 min. Mass spectrometry conditions: AB SCIEX QTRAP 7500, detection in positive/negative mode, Curtain Gas (CUR) 45, Collision Gas (CAD) Medium, IonSpray Voltage (IS) + 4500/-4500, Temperature (TEM) 550, Ion Source Gas 1 (GS1) 50, Ion Source Gas 2 (GS2) 50. Draw a linear regression standard curve with the mass spectrometric peak area of the analyte on the y-axis and the concentration of the analyte on the x-axis to calculate the concentration results.

Non-targeted measurement and analysis of metabolites

Approximately 100 mg of each sample was placed into a 2 mL centrifuge tube, and metabolites were extracted using 800 µL of extraction solvent (methanol: water = 4:1, v/v) containing four internal standards, including L-2-chlorophenylalanine (0.02 mg/mL). Samples were homogenized in a cryogenic tissue grinder for 6 min (– 10 °C, 50 Hz), followed by cold ultrasonic extraction for 30 min (5 °C, 40 kHz). The extracts were then incubated at – 20 °C for 30 min and centrifuged at 13,000 × g for 15 min at 4 °C.

Fig. 6 Grafted seedlings of *C. oleifera* on shoot-flushing (branch) and non-flushing (bud) plants

The supernatant was transferred into an autosampler vial with an insert for LC-MS analysis. A quality control (QC) sample was prepared by pooling equal volumes of all sample extracts to assess the reproducibility of the entire analytical process. LC-MS analysis was performed on a Thermo Fisher Scientific UHPLC-Q Exactive system (ultra-high-performance liquid chromatography coupled with quadrupole–Orbitrap high-resolution mass spectrometry). Chromatographic separation was carried out on a BEH C18 column (100 mm × 2.1 mm i.d., 1.7 µm) with an injection volume of 3 µL. Mobile phase A consisted of 2% acetonitrile in water (with 0.1% formic acid), and mobile phase B was acetonitrile (with 0.1% formic acid). Raw data were processed using Progenesis QI (Waters Corporation, Milford, USA) to generate a data matrix. Principal component analysis (PCA) was performed using the ropls package (version 1.6.2). Significantly differentially abundant metabolites were defined based on the OPLS-DA model with VIP > 1, $p < 0.05$, and |fold change|> 1. Pathway enrichment analysis was conducted using the Python package scipy.stats via Fisher's exact test. Metabolomics pathway enrichment analysis was performed, and *p*-values were adjusted for multiple testing using the Benjamini–Hochberg false discovery rate (FDR) method.

Library construction and transcriptome analysis

Total RNA was extracted from tissue samples using the TRIzol reagent kit. RNA concentration and purity were assessed with a NanoDrop 2000 spectrophotometer, RNA integrity was verified by agarose gel electrophoresis, and the RNA Integrity Number (RIN) was determined using an Agilent 2100 Bioanalyzer. Only samples with RIN > 6.5 and OD260/280 ratios between 1.8 and 2.2 were used for subsequent analyses. Stranded mRNA libraries were constructed using the Illumina® Stranded mRNA Prep, Ligation method. Sequencing of the cDNA libraries was performed on the NovaSeq X Plus platform. The raw sequencing data have been deposited in the National Genomics Data Center under the BIG Sub database (BioProject accession: PRJCA040565,). Quality control of raw reads was conducted using fastp software [35]. High-quality clean reads were aligned to the reference genome [36] using HiSat2 [37], and gene expression levels were quantified using RSEM [38]. Differentially expressed genes (DEGs) were identified with DESeq2 [39] using thresholds of $|\log_2 FC| > 1$ and *adjusted p-value* < 0.05. Functional enrichment analyses, including Gene Ontology (GO) and Kyoto Encyclopedia of Genes and Genomes (KEGG) pathway enrichment, were performed using the clusterProfiler v4.8.1 R package [40]. Weighted Gene Co-expression Network Analysis (WGCNA v1.72.1) [41] was applied to construct co-expression modules using all DEGs that had an FPKM > 5 in at least one sample. Other WGCNA parameters were set as follows: minModuleSize = 30 and MEDissThres = 0.25. Based on the identified DEGs and differentially abundant metabolites, shared metabolic pathways were determined through KEGG enrichment analysis. Pearson correlation coefficients were calculated between DEGs and

metabolites, and gene–metabolite pairs with |correlation coefficient| ≥ 0.6 and p-value < 0.05 were selected for downstream integrative analysis.

RT-qPCR validation

Eight differentially expressed genes were selected, and RT-qPCR was performed using *GAPDH* as the reference gene to validate the reliability of the transcriptome data. PCR primers were designed using Primer 5.0. The RT-qPCR reaction mixture (20.0 μL total volume) contained 2.0 μL cDNA template, 0.4 μL each of forward and reverse primers, 10 μL of 2× PerfectStart Green qPCR SuperMix, and RNase-free water to bring the final volume to 20 μL. The thermal cycling conditions were as follows: an initial denaturation at 95 °C for 1 min, followed by 40 cycles of 94 °C for 5 s (denaturation) and 60 °C for 15 s (annealing/extension). Relative expression levels were calculated using the $2^{-\Delta\Delta Ct}$ method.

Supplementary Information

The online version contains supplementary material available at https://doi.org/10.1186/s12864-026-12702-1.

Supplementary Material 1.

Acknowledgements

Not applicable.

Authors' contributions

Conceptualization, Y. Zhu and Ch. Xu; methodology, Y. Zhu and F.Xiao; software, F.Xiao and Y.Zhu; validation, Y. Zhu, Ch. X, F.Li, J. Xu, and Q. Zeng; formal analysis, Y. Zhu, Ch. X and F.Xiao; investigation, Y. Zhu, Y.Wei and Q.zeng; resources, Y. Zhu, F. Xiao; data curation, Y. Zhu, Ch. X and F.Xiao; writing—original draft preparation, Y. Zhu ; writing—review and editing, F.Xiao and J. Xu.; visualization, Y. Zhu and Ch Xu; supervision, Y. Zhu; project administration, Y. Zhu; funding acquisition, J. Xu. All authors have read and agreed to the published version of the manuscript.

Funding

This research was funded by the Forestry Bureau of Guizhou Projects (grant number: Qianlinkehe[2026]zhongdian 008 and Gui[2025]TG2), Science and Technology Department of Guizhou Province (grant number: Qiankehejichu-ZK[2024]zhongdian 091, and Qiankefuqi [2018]4003).

Data availability

The raw sequence data reported in this paper have been deposited in the Genome Sequence Archive in National Genomics Data Center, China National Center for Bioinformation / Beijing Institute of Genomics, Chinese Academy of Sciences (BioProject accession: PRJCA040565) that are publicly accessible at https://ngdc.cncb.ac.cn/gsa.

Declarations

Ethics approval and consent to participate

All plants samples were collected on improved variety base, we had obtained the permissions from that unit. Experimental research and field studies on plants including the collection of plant material are comply with relevant guidelines and regulation. All samples were identified by Yayan Zhu and Jie Xu, and all voucher specimens were deposited in the Guizhou Academy of Forestry (voucher ID numbers: CoCL40 for *Camellia oleifera*, CmLP11 for *Camellia meiocarpa*, CwWP1 for *Camellia weiningensis*).

Consent for publication

Not applicable.

Competing interests

The authors declare no competing interests.

Received: 1 December 2025 / Accepted: 24 February 2026
Published online: 03 March 2026

References

1. Xu J, Lu Y, Deng Z, Ban Q, Deng Z. Practical techniques for rootstock treatment in top-grafting of *Camellia oleifera*. Guizhou Sci Technol. 2023;51:20–3. https://doi.org/10.16709/j.cnki.gzlykj.2023.03.007.
2. Yang B, Li F, Chen Y, Zhang M, Wang G. Study on the configuration of main cultivated varieties of *Camellia oleifera* in the low hilly areas of eastern Guizhou. Guizhou Forestry Sci Technol. 2024;52:5–10. https://doi.org/10.16709/j.cnki.gzlykj.2024.01.016.
3. Wei Z. Key techniques and influencing factors in grafting seedling production of *Camellia oleifera* using bud-rootstock. South Agric. 2021;15:54–5. https://doi.org/10.19415/j.cnki.1673-890x.2021.02.025.
4. Wei R. Research on grafting propagation techniques for *Camellia oleifera*. Contemp Agricultural. 2024;108:104–5.
5. Long W, Yao X, Wang K, Wang Y. Compatibility analysis of scion–rootstock combinations in common *Camellia oleifera*. J Jiangxi Agricultural Univ. 2013;35:346–51. https://doi.org/10.13836/j.jjau.2013061.
6. Ge X, Zhong Q, Tan X, Wang J, Cao L, Zhou Y, et al. Integrated multi-omics analysis to elucidate the role of shikimic acid and phenethylamine in the effect of scions on rootstocks of *Camellia oleifera*. Ind Crops Prod. 2023;203:117222. https://doi.org/10.1016/j.indcrop.2023.117222.
7. Wang X, Wang R, Chen L, Tang W, Peng Y, Peng S, et al. Compatibility analysis of scion–rootstock combinations in bud-grafting of new *Camellia oleifera* cultivars. J Cent South Univ Forestry Technol. 2017;37:1–6. https://doi.org/10.14067/j.cnki.1673-923x.2017.12.001.
8. Wang Z, Liao H, Hu D, Xu J, Xu A, Liu H. Effects of rootstock and scion cultivars on the morphology of bud-grafted *Camellia oleifera* seedlings. J Jiangxi Agricultural Univ. 2021;43:126–35. https://doi.org/10.13836/j.jjau.2021014.
9. Xu C, Zhou X, Du Y, Zeng B, Cheng J, Cheng X. Effects of different types of scion wood on the growth and development of bud-grafted Camellia oleifera seedlings. Hubei Forestry Sci Technol. 2011;22:15–8.
10. Zhang M, Lan F, Chen J, Zhou H, Huang D, Song X, et al. Key techniques for bud-grafting propagation of *Camellia oleifera*. Forestry Sci Technol Dev. 2014;28:127–30. https://doi.org/10.13360/j.issn.1000-8101.2014.05.032.
11. Lin Y. Preliminary report on bud-grafting propagation experiments of *Camellia oleifera*. Jiangxi Forestry Sci Technol. 2011;28–30. https://doi.org/10.16259/j.cnki.36-1342/s.2011.04.019.
12. Long W, Yao X, Wang K, Lin P, Dou P. Effect of bud position on scion wood on grafting propagation of *Camellia oleifera*. Forestry Sci Technol Dev. 2012;26:62–6.
13. Domagalska MA, Leyser O. Signal integration in the control of shoot branching. Nat Rev Mol Cell Biol. 2011;12:211–21. https://doi.org/10.1038/nrm3088.
14. Liu J, Fu K, Li B, Wang Q, Cao Y, Zhan Y. A novel approach for enhancing sprouting to increase yield and its mechanism in *Fraxinus mandshurica* Rupr. Sci Hortic. 2025;339:113897. https://doi.org/10.1016/j.scienta.2024.113897.
15. Iwase A, Harashima H, Ikeuchi M, Rymen B, Ohnuma M, Komaki S, et al. WIND1 promotes shoot regeneration through transcriptional activation of Enhancer of Shoot Regeneration1 in arabidopsis. Plant Cell. 2017;29:54–69. https://doi.org/10.1105/tpc.16.00623.
16. Physiological. anatomical and transcriptome analyses reveal 'huaizhi' as widely compatible rootstock in litchi chinensis sonn. grafting. Sci Hortic. 2024;331:113161. https://doi.org/10.1016/j.scienta.2024.113161.
17. Zhu Y, Xu J, Wang G, Xiao F, Zhang M, Zeng Q, et al. Integrated metabolome and transcriptome analyses provides insights into ovule abortion in *Camellia oleifera*. Plants (basel Switz). 2025;14:613. https://doi.org/10.3390/plants14040613.
18. Gao Z, Chen Z, Wang J, Liu W. Integrated transcriptome and metabolome analysis revealed mechanism underlying anthocyanin biosynthesis during flower color formation in lagerstroemia indica. Horticulturae. 2024;10:1229. https://doi.org/10.3390/horticulturae10111229.

19. Si C, Yang S, Sun Z, Zhang G, Zhong Q. Dissecting flavonoid metabolic differences in pepino (*Solanum muricatum*) fruit using integrated transcriptomic and metabolomic analyses. Acta Agriculturae Boreali-Sinica. 2023;38:53–62.
20. Gao G. Dissecting the molecular mechanism of maize resistance to southern leaf blight based on transcriptomic and metabolomic analyses. Master's thesis. Zhengzhou: Henan Agricultural University; 2024.
21. Sun M, Lai Z, Zhou R, Zhou M, Yin Y, Zhao D, et al. An AUX/IAA gene PlIAA9 regulates lignin deposition during secondary growth of herbaceous peony (*Paeonia lactiflora* Pall.) stems. Sci Hort. 2025;342:114003. https://doi.org/10.1016/j.scienta.2025.114003.
22. Li C, Wang H, Ye Y, Chen Y, Ren H, Li Y, et al. Study on the regulatory role of plant hormones in the spring shoot growth and development of *Camellia sinensis*. J Tea Sci. 2023;43:335–48. https://doi.org/10.3969/j.issn.1000-369X.2023.03.004.
23. Zhang J, Ye T, Chen Y, Li Y, Wang D, Luo J, et al. Effects of exogenous hormone treatment of scions on top-grafting of *Camellia oleifera* in Hainan. Nonwood For Res. 2020;38:53–9. https://doi.org/10.14067/j.cnki.1003-8981.2020.02.007.
24. Yao C, Finlayson SA. Abscisic acid is a general negative regulator of arabidopsis axillary bud growth. Plant Physiol. 2015;169:611–26. https://doi.org/10.1104/pp.15.00682.
25. Song W, Ma X, Tan H, Zhou J. Abscisic acid enhances resistance to alternaria solani in tomato seedlings. Plant Physiol Biochem: PPB. 2011;49:693–700. https://doi.org/10.1016/j.plaphy.2011.03.018.
26. Müller D, Leyser O. Auxin, cytokinin and the control of shoot branching. Ann Bot. 2011;107:1203–12. https://doi.org/10.1093/aob/mcr069.
27. Wolters H, Jürgens G. Survival of the flexible: Hormonal growth control and adaptation in plant development. Nat Rev Genet. 2009;10:305–17. https://doi.org/10.1038/nrg2558.
28. Azizi P, Rafii MY, Maziah M, Abdullah SNA, Hanafi MM, Latif MA, et al. Understanding the shoot apical meristem regulation: A study of the phytohormones, auxin and cytokinin, in rice. Mech Dev. 2015;135:1–15. https://doi.org/10.1016/j.mod.2014.11.001.
29. Zhong W, Chai Y, Zhang K, Chen X, Lu K, Tao L. Research on cytochrome P450 enzymes in the phenylpropanoid metabolic pathway. J Anhui Agricultural Sci. 2008;5285–9. https://doi.org/10.13989/j.cnki.0517-6611.2008.13.005.
30. Chakraborty P, Biswas A, Dey S, Bhattacharjee T, Chakrabarty S. Cytochrome P450 gene families: Role in plant secondary metabolite production and plant defense. J Xenobiot. 2023;13:402–23. https://doi.org/10.3390/jox13030026.
31. Li M, Yang Y, Xiao H, Yuan Z, Zhou H. Advances in the involvement of plant cytochrome P450 enzymes in the biosynthesis of monoterpenoids. Chem Bioeng. 2025;42:8–17.
32. Zhou Z, Feng J, Huo J, Qiu S, Zhang P, Wang Y, et al. Versatile CYP98A enzymes catalyse meta-hydroxylation reveals diversity of salvianolic acids biosynthesis. Plant Biotechnol J. 2024;22:1536–48. https://doi.org/10.1111/pbi.14284.
33. Karamat F, Olry A, Doerper S, Vialart G, Ullmann P, Werck-Reichhart D, et al. CYP98A22, a phenolic ester 3'-hydroxylase specialized in the synthesis of chlorogenic acid, as a new tool for enhancing the furanocoumarin concentration in ruta graveolens. BMC Plant Biol. 2012;12:152. https://doi.org/10.1186/1471-2229-12-152.
34. Zhang B, Lewis KM, Abril A, Davydov DR, Vermerris W, Sattler SE, et al. Structure and function of the cytochrome P450 monooxygenase cinnamate 4-hydroxylase from sorghum bicolor. Plant Physiol. 2020;183:957–73. https://doi.org/10.1104/pp.20.00406.
35. Chen S, Zhou Y, Chen Y, Gu J. fastp: An ultra-fast all-in-one FASTQ preprocessor. Bioinform (oxf Engl). 2018;34:i884–90. https://doi.org/10.1093/bioinformatics/bty560.
36. Lin P, Wang K, Wang Y, Hu Z, Yan C, Huang H, et al. The genome of *Camellia oleifera* and population genomics analysis provide insights into seed oil domestication. Genome Biol. 2022;23:14. https://doi.org/10.1186/s13059-021-02599-2.
37. Kim D, Langmead B, Salzberg SL. HISAT: A fast spliced aligner with low memory requirements. Nat Methods. 2015;12:357–60. https://doi.org/10.1038/nmeth.3317.
38. Li B, Dewey CN. RSEM: Accurate transcript quantification from RNA-seq data with or without a reference genome. BMC Bioinf. 2011;12:323. https://doi.org/10.1186/1471-2105-12-323.
39. Love MI, Huber W, Anders S. Moderated estimation of fold change and dispersion for RNA-seq data with DESeq2. Genome Biol. 2014;15:550. https://doi.org/10.1186/s13059-014-0550-8.
40. Wu T, Hu E, Xu S, Chen M, Guo P, Dai Z, et al. clusterProfiler 4.0: A universal enrichment tool for interpreting omics data. Innovation. 2021;2:100141. https://doi.org/10.1016/j.xinn.2021.100141.
41. Langfelder P, Horvath S. WGCNA: An R package for weighted correlation network analysis. BMC Bioinf. 2008;9:559. https://doi.org/10.1186/1471-2105-9-559.

Publisher's Note